Adsorption Kinetics of Basic Blue-41 Dye on Synthetic Foam-Shaped Zeolite ZSM-5

Labidi Nouar Sofiane

* labidi19722004@yahoo.fr

Department of Matter Sciences, Faculty of Sciences and Technology, University of Tamanghasset 11000. Algeria.

Abstract: *The synthesized foam-shaped zeolite ZSM-5 material was characterized by X-ray diffraction (XRD), (FTIR) spectroscopy, scanning electron microscopy (SEM) and BET techniques. The adsorption performance of the material were evaluated for the basic blue-41 dye removal. A maximum removal amount of 161.29 mg/g at 323K was achieved. Experimental kinetic data of this new adsorbent fitted well with the pseudo-second order model. The apparent diffusion coefficient values was in the range of 10^{-12} cm^2/s. The regeneration tests revealed that the adsorption efficiency of the foam-shaped zeolite sample was retained after three regeneration runs, with a loss of only 6% of the original adsorbed value.*

Keywords: zeolite ZSM-5, basic blue-41, adsorption, diffusion coeffient, adsorption energy, regeneration.

1. INTRODUCTION

The most important family members of crystalline microporous solids are zeolites. These solids have multiple industrial applications, they are used as desiccants to protect moisture sensitive items and as water softeners, in particular in washing powders. These solids are also very important in hetero- geneous catalysis and more particularly in petroleum refining processes to convert heavy fractions into gasoline or gas (FCC catalytic cracking) [1-4]. Zeolites are silicates or aluminosilicates whose sequencing in the space of tetrahedra (TO_4) can lead to the production of a large number of different open structures. Zeolites have cavities and channels, with openings ranging from 4 to 15 Å. Because of this, these materials are also often referred to molecular sieves since some molecules can penetrate into the structure while others of larger diameter are excluded [4].

Zeolite materials are usually obtained by heating an alkaline solution of sodium silicate and sodium aluminate [4, 5]. The type of zeolite formed depends on the conditions: (i) the reactants used, (ii) the synthesis conditions applied (such as temperature, time, and pH), and (iii) the templating ion.

The foam zeolite is an ZSM-5 zeolite type, which is an alumino-silicate material with a high silica and low aluminum content. Its internal structure is based on channels with intersecting tunnels. This zeolite has been selected due to its interest in the separation applications process [4-7].

Despite wide interest in these materials in industrial circles [8-13], there are few suitable experiments that provide a basic exposure to the field. Therefore, an experiment is described for the synthesis of the foam zeolite ZSM-5 with an open-cell and microcellular structure [6]. In the best of our knowledge, significant work has been done on the synthesis and characterization of zeolites and its application in a particular field [14-19]. Nevertheless a paper specifically focusing on the synthesis of foam zeolite (ZSM-5) and its implication in the removal of basic dyes has been published.

The purpose of this study is the synthesis and characterization of a new foam-shaped zeolite ZSM-5 material, thus, its efficiency as a removal agent for basic blue-41 textile dye. The adsorption experiments of basic blue-41 were performed in batch by controlling different parameters, such as solution pH of the, initial concentrations and temperature. The experimental data were modeled with various kinetic models to find the most suitable model.

2. EXPERIMENTAL PROCEDURE

2.1. Materials

Sodium aluminate (Sigma-Aldrich, Al_2O_3 50-

56%, Na$_2$O 40-45%) and tetraethyl orthosilicate (TEOS) (Aldrich, 98%) is used to generate amuninosilicate solution. The tetrapropylammonium hydroxide (TPAOH) (Fluka, ~20% in distilled water) is employed as a source of template.

Bsic Blue-41(Sigma-Aldrich) has the molecular formula C$_{20}$H$_{26}$N$_4$O$_6$S$_2$ and molecular weight of 482.57 g/mol. The Molecular Structure of the BB-41 used as adsorbate is given in Fig.1.
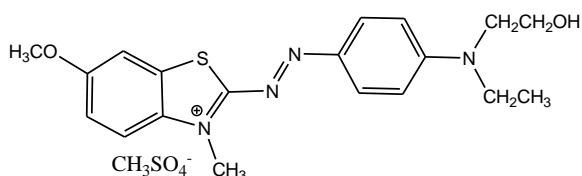

Fig. 1. Molecular Structure of the cationic basic bleu-41 (BB-41).

2.2. Synthesis of Zeolite ZSM-5

The method used for the synthesis of the foam zeolite ZSM-5 is similar to the one reported by Saini et al [6]. A solution of 10 mL (1 M) tetrapropylammonium hydroxide (TPAOH) (Fluka, ~20% in water) with 49 mL of distilled water is prepared in 100 mL flask. To this solution, 17 g of Tetraethyl orthosilicate (TEOS) (Aldrich, 98%) is slowly added and stirred for 15 minutes. In the meanwhile, 1 M solution of sodium aluminate (Sigma-Aldrich, Al$_2$O$_3$ 50-56%, Na$_2$O 40-45%) is prepared and 3.2 mL of this solution is added to the stirring mixture slowly. This new mixture is then stirred for next 2 hrs, at room temperature, and then transferred into 100 mL glass bottle that already contains a cylindrical polyurethane foam template. The bottle is closed and kept in an oven at 120°C until next day. On next day, a monolith light inorganic material is obtained. This monolith has a pale yellow appearance, due to presence of un-decomposed polyurethane foam fragment remained in structure, which were then removed by, washing with excess of water and acetone, and then calcined in tubular oven, preferably with flowing air, at 550°C for at least 2 h. It is important to note here, that a sudden rise in oven temperature may cause cracks in prepared foam, it is therefore advised that temperature should be increased with a ramp/rate of 10°C/min. After calcination, the sample turns into bright white colored foam. Once the oven returns to

temperature 100-80°C the sample contained therein can be removed, weighted, and used forthwith for further adsorption-capacity measurement [6, 7]. The synthetic pathway is presented in Fig.2.
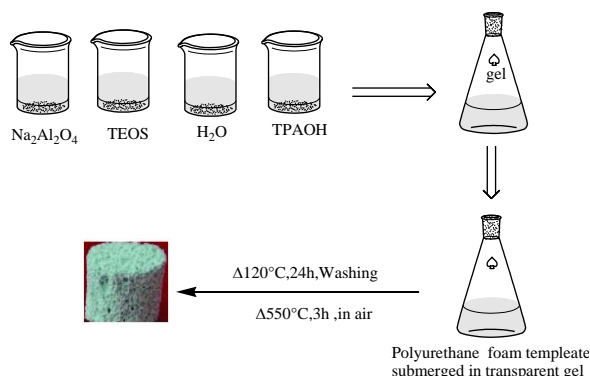
Fig. 2. Route synthesis of zeolite ZSM-5 in presence of polyurethane foam template.

2.3. Zeolite Characterization.

X-ray diffraction (XRD) of product was carried out with a BRUKER AXS x-ray diffractometer. Specific surface area was determined through N$_2$ adsorption/desorption isothermal tests (AutosorbiQ1-MP). Morphology was observed by PHILIPS(X130, SEM). Fourier transformation infrared (FTIR) was run on JASCO 460 infrared spectrometer, the wavelength range is 400 cm^{-1}-4000 cm^{-1}, and resolution is 4 cm^{-1}.

2.4. Adsorption experiments

Batch adsorption experiments were carried to measure the amount adsorbed of BB-41 onto foam zeoliteZSM-5. In general, 0.1 g adsorbent was incubated in 50 mL BB-41 solution of desired initial concentration at a solution pH= 7 and a temperature of 25°C under constant stirring (300rpm). Adsorption experiments were performed at initial basic blue concentration of 50, 100, 200 and 300 mg.L^{-1}.

The basic blue adsorption kinetics on zeoliteZSM-5 was evaluated at different concentrations (50, 100, 200 and 300 mg.L^{-1}) at programmed time intervals between 5 and 90 min. The solid and liquid phases were separated using a syringe filter after equilibrium, and the concentration of residual dye was determined at λ$_{max}$= 610 nm. The adsorption equilibrium was determined according to the equation below (Eq. 1) [20]:

$$q_e = \frac{C_0 - C_e}{m} \times V \qquad (1)$$

where q_e is the amount adsorbed (mg.g^{-1}); C_o is the initial dye concentration (mg.L^{-1}); C_e is the equilibrium concentration of (mg.L^{-1}); C_t is the dye solution concentration at time, t (mg.L^{-1}); m is mass of the adsorbent (g); and V is the volume of dye solution (L). When t is equal to the equilibrium time $C_t = C_e$ and $q_t = q_e$, then the amount of dye adsorbed at equilibrium, q_e, can be calculated by q_t.

2.5. Regeneration Tests

With the aim of exploring the potential reutilization of zeoliteas a adsorbent for the reoval basic blue dye, the zeolithe ZSM-5 was heated at 500°C for 2 h. This calcined product was employed to repeat the adsorption process within an adsorbent mass of 0.1 g, 50 mL of BB-41 at 700 mg.L^{-1}, pH= 7 and a temperature of 25°C under constant stirring at 300 rpm. The dye-laden zeolitewas affirmed by UV−vis spectroscopy (UV mini- 1240) [21].

3. RESULTS AND DISCUSSION

3.1. Zeolites characterization

3.1.1. X-ray Diffraction (XRD)

The XRD results of the synthesized zeoliteis shown in Fig.3. It can be seen that the synthesized zeolite have typical characteristic peaks near 2θ= 7.7°, 16.3°, 24.50° and 27. 5°. The XRD peaks of the product are well matched with diffraction peaks ascribed to ZSM-5 reference pattern (JCPDS 44-0003) [22, 23].
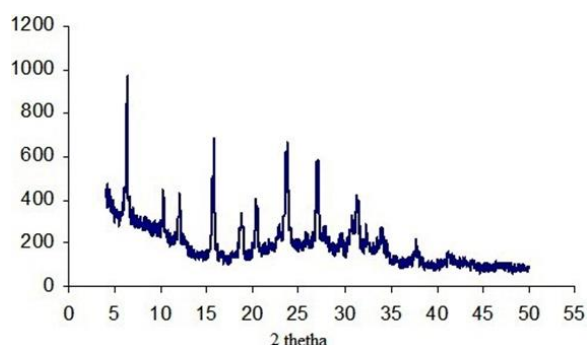

Fig. 3. XRD pattern of the synthesized foam-shaped zeolite.

3.1.2. MEB and BET Results

The SEM image of the synthesized zeolite ZSM-5 is shown in Fig.4. The surface of the foam zeolite ZSM-5 is relatively smooth and contains many pores and are similar to that of traditional zeolite from those reported by Feng et al [23].
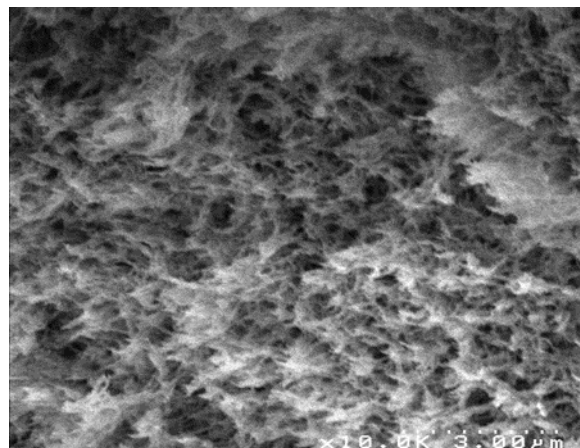

Fig. 4. SEM micrograph of the synthesized foam-shaped zeolite ZSM-5.

The BET (Brunauer, Emmett and Teller) equation was used to estimate the specific surface area (S_{BET}) [24]. The sample in Fig. 5, showed a Langmuir isotherms (type I), indicating microporous characteristics. The specific surface area is 364 m^2.g^{-1} for the synthesized foam zeolite ZSM-5. The apparent bulk density determined by the external volume of samples for our zeolite-foam at 100°C is 0.014 g.cm^{-3}.
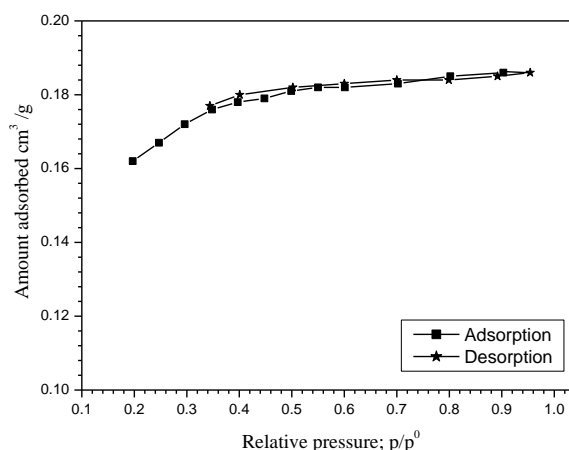

Fig. 5. N$_2$ adsorption-desorption isotherms at 77 K for the synthesized zeolite ZSM-5.

3.1.3. FTIR Spectrum

The FTIR results of ZSM-5 is shown in Fig. 6. The characteristic skeleton vibration peaks of ZSM-5 zeolite are around 1225 cm^{-1}, 1047 cm^{-1}, 970 cm^{-1}, 556 cm^{-1} and 456 cm^{-1}. Besides, there is

a binding vibration peaks of water molecules near 1642 cm^{-1} and an O–H stretching vibration peak at 3490 cm^{-1}, which are caused by water in the zeolite. The FTIR spectra for ZSM-5 is consistent with those reported by Pan et al [25].
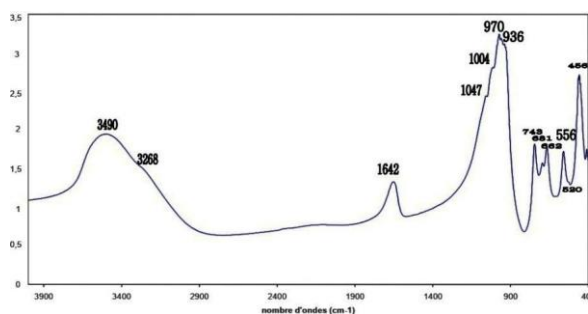
Fig. 6. FTIR Spectra of the synthesized foam-shaped zeolite ZSM-5.

3.2. Adsorption equilibrium and kinetic analysis

Equilibrium studies of basic blue-41 adsorption were performed at initial concentrations of 50, 100, 200 and 300 mg.L^{-1}. As can be observed in Fig.7, the plots of adsorbed amounts q_t versus contact time show that the maximum sequestration of dye was observed within 30 min. The synthesized foam-shaped zeolite ZSM-5 exhibited adsorption capacities at initial dye concentrations of 50, 100, 200 and 300 mg.L^{-1} close to 3.17, 16.60, 33.05 and 49.65 mg.g^{-1}, respectively. The aforementioned adsorption capacity is relatively higher in comparison to several reported adsorbents in the literature. The faster adsorption kinetics could be attributed to quick diffusion of dye molecules into the zeoliteframework, which results from the porous nature as well as the the mixture speed of stirring [34].

The kinetic adsorption characteristics of BB-41 onto the foam-shaped zeolite ZSM-5, was determined by the linear form of the pseudo-first-order and pseudo-secondorder model expressed in Eqs. 2 and 3, respectively [20].

$$\frac{1}{q_t} = \frac{1}{q_e} + \left(\frac{K_1}{q_e}\right) \times \left(\frac{1}{t}\right) \tag{2}$$

$$\frac{t}{q_t} = \frac{1}{K_2 q_e^2} + \left(\frac{1}{q_e}\right)t \tag{3}$$

where q_e and q_t (mg.g^{-1}) are the adsorption capacity of BB-41 onto the adsorbent at equilibrium and time t(min), respectively, and

K_1(min^{-1}) and K_2 (g. mg^{-1}. min^{-1}) are the first- and second-order rate constant, respectively. The kinetic rate constant K_1 and q_e (eq. 2) were deduced from the plots of 1/ q_t versus 1/t in Fig. 8a. K_2 and qe (eq. 3) are obtained by plotting t/q_t versus t in Fig. 8b.
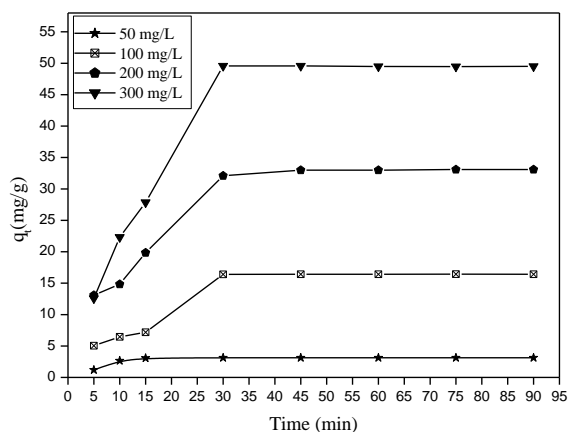
Fig. 7. Effect of contact time on the removal of BB-41 by the foam-shaped zeolite ZSM-5 (T= 298 K, pH= 7, agitation speed= 300 rpm and amount of zeolite= 0.1 g).

The values of the kinetic rate constant, adsorption capacities $q_{e,cal}$, $q_{e,exp}$ and the correlation coefficient (R^2) are presented in Table 1.

Fig.8a showed the pseudo-first order adsorption kinetics for BB-41 onto the synthezised foam-shaped zeolite ZSM-5. It was observed for the pseudo-first-order model shown in Figure 8, a large disagreement between the experimental ($q_{e,exp}$) and calculated ($q_{e,cal}$) values of the equilibrium adsorption capacities. The calculated values of the correlation coefficient R^2 are 0.843, 0.906, 0.964 and 0.480, respectively. Moreover, the values of the calculated rate constant K_1 increased with increasing the BB-41 concentrations from 50 mg.L^{-1} to 100 mg.L^{-1} and also from 200 mg.L^{-1} to 300 mg.L^{-1}. This observation suggest that adsorption of BB-41 dye on the the synthezised foam-shaped zeolite ZSM-5 does not obey the pseudo-first-order mode.

The linear form of the pseudo-second-order is presented in Fig. 9b. As can be observed from (Fig. 8b), the adsorbed quantity at equilibrium $q_{e,cal}$ increases with an increase in initial dye concentration, while the kinetic rate constant K_2 decreases. In addition, the values of experimental adsorption capacities ($q_{e,exp}$) are found to be very close to those of the calculated ($q_{e,cal}$) values. The values of the correlation coefficient R^2 for the

linearized form of the pseudo-second-order model are higher than 0.95, the pseudo-second-order model was better than that for the pseudo-first-order (Table 1), hence indicating an adequate model to correctly describe the adsorption kinetics. It can be concluded that the adsorption of BB-41 dye onto zeolitewas likely a second order reaction. . Similar results are found in the adsorption of BB-41 onto different adsorbents such as a Aluminum and zirconium intercalated clay [26], Waste brick materials [27], activated carbon [28] and black tea leaves [29].

The intraparticle diffusion model in equation (Eq. 4) is also used to analyze the diffusion mechanism [20]:

$$q_t = K_p t^{1/2} + C \qquad (4)$$

where q_t is the adsorption capacity (mg.mg^{-1}), K_p is the intraparticle diffusion rate constant (g.mg^{-1}.min$^{-1/2}$) and C (mg.mg^{-1}) is a constant that provides information regarding the thickness of the boundary layer. A plot of fraction of solute adsorbed against $t^{0.5}$ can be used to estimate the intraparticle diffusion rate in the linear range.

The values of the diffusion coefficient (D_i) are deduced from the following formula [20]:

$$D_i = \frac{0.03 \times r_0}{t^{1/2}} \qquad (5)$$

where $t^{1/2}$ is a half- time reaction (s) (adsorption equilibrium reaction), r_0 is the particle diameter of the adsorbent in (cm), and D is intraparticle diffusion parameter (cm^2/s).

Fig. 9 presents the plots of q_t versus $t^{1/2}$ for the BB-41 dye concentrations of 50, 100, 200 and 300 mg/L. The values of the external diffusion constant K_p, diffusion coefficients (D; cm^{2}s^{-1}) and correlation coefficients R^2 are listed in Table 2.

The regression estimates data in Table 2, generates straight lines wich does not pass through the origin, suggesting that the intraparticle diffusion is not the rate controlling step in the adsorption process. The intraparticle diffusion constants K_p (g.mg^{-1}.min$^{-1/2}$) is observed to have decreasing values, which are directly related to the nature of the internal porosity of zeolite [30]. The values of the intercept (C mg.mg^{-1}) increase with the initial concentration of the dyes, indicating an increase in the thickness of the boundary layer.
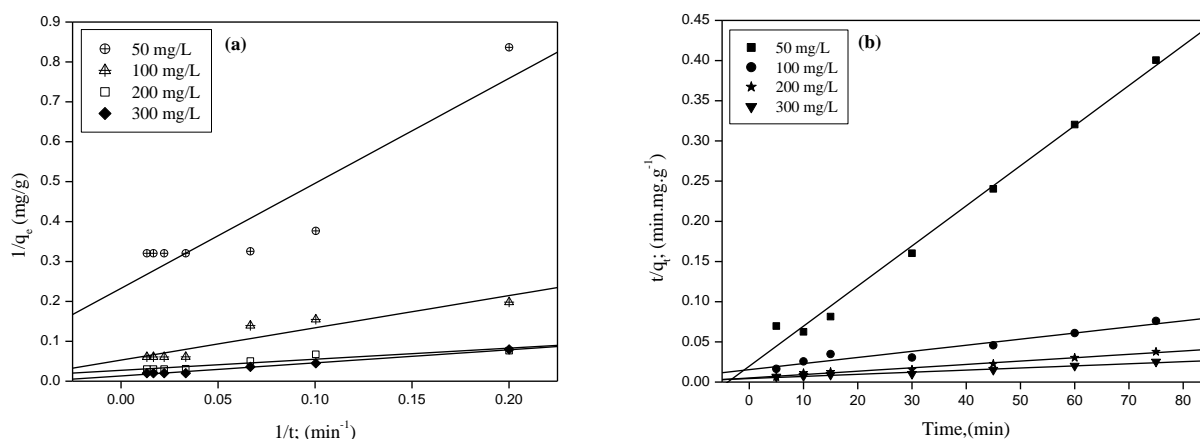

Fig. 8. Plots of (a) pseudo-first-order kinetics, (b) pseudo-second-order kinetics models of basic blue onto zeolite ZSM-5 (0.1 g adsorbent dose, T= 298 K and pH= 7).

Table 1. Parameters of kinetic models for BB-41 adsorption onto foam-shaped zeolite ZSM-5 at different initial dye concentrations (C_0) (pH 7.0; temp= 298 K; volume= 50 mL; material mass= 100 mg and agitation 300 rpm).

	Pseudo-first-order kinetics				Pseudo-second-order kinetics			
C_0 (mg/l)	K_1 (min^{-1})	($q_{e,cal}$) (mg/g)	R^2	χ^2	K_2 (g/mg min)	($q_{e,cal}$) (mg/g)	R^2	χ^2
50	11.33	4.31	0.852	0.302	0.0753	3.34	0.990	0.134
100	15.54	19.23	0.888	0.360	0.0022	22.22	0.956	0.345
200	10.26	37.04	0.892	0.430	0.002	40.00	0.982	0.278
300	25.15	76.92	0.990	9.668	0.0009	66.67	0.970	0.963

This indicats also, that intraparticle diffusion is not the only rate limiting step, but other kinetic processes may control the adsorption rate, all of which may be operating simultaneously.
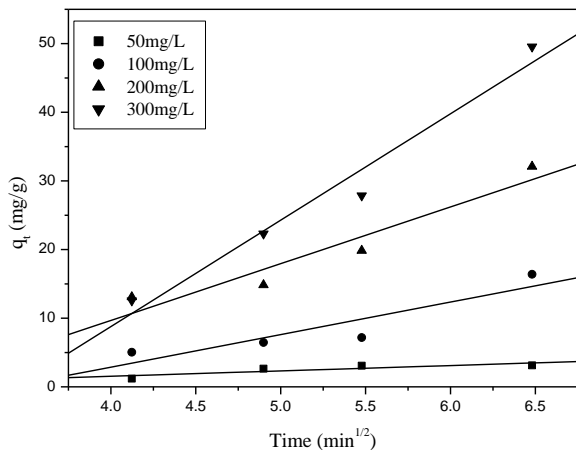
Fig. 9. Intraparticle-diffusion model for BB-41 adsorption onto zeolite ZSM-5: (T= 298 K, 0.1 g adsorbent dose, agitation= 300 rpm, pH= 7 and volume= 50 mL).

It was observed in Table 2, that an increase in the initial dye concentration decreases the BB-41 diffusion rate parameters. This can be explained by an increase of the driving force leading to an increases of the diffusion rate of the dye molecules onto zeolite ZSM-5 pores. The values of diffusion coefficient show that the relation between initial dye concentration and the effective diffusion coefficient, Di, has the same trend as the intraparticle diffusion rate constant K_p, and this trend may be related to the increasing agglomeration of BB-41 with the increase of its concentration. The values of the effective diffusion parameter (Di) was estimated to be of the order of (12 cm^2/s). It is reported that the values of the diffusion coefficient in the range of (1.21×10^{-10} to 2.12×10^{-11}) indicates an intraparticle diffusion as the rate-limiting step in the adsorption process. Our results are in agreement to the data obtained in the literature [30].

3.2.1. Regeneration proprety:

The regeneration process is an important factor for the feasibility of the removal process, and it will add value to the used materials. Fig.10 presents the experimental results of the adsorption amount in the first four adsorption–regeneration cycles for zeolite material. The results obtained in Fig.10, indicated that the BB-41 uptake is dcreased by a percentage of 3%, 6% and 30% for the second run, third run and the fourth run, respectively. The zeolite ZSM-5 exhibited sustainable removal properties after three cycles of reuse. It could be concluded that zeolite ZSM-5 could be completely recycled after being used as potential adsorbent for basic blue-41 contaminated water.
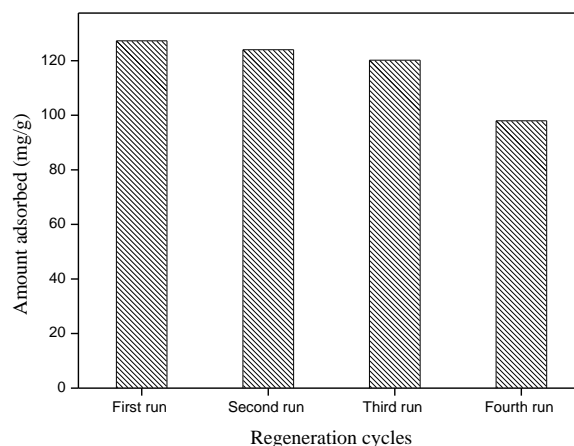
Fig. 10. Regeneration properties of zeolite ZSM-5.

4. CONCLUSIONS

In summary, the zeolite ZSM-5 sample was synthesized in the presence of polyurethane foam template. The prepared material had high surface area of 364 m^2.g^{-1} and an apparent bulk density at 100°C of 0.014 g·cm^{-3}. The resulting foam-shaped zeolite ZSM-5 material showed an excellent adsorption ability towards the basic blue-41 dye. The adsorption kinetic followed the pseudo-second-order model.

Table 2. Intraparticle-diffusion parameters and diffusion coefficients for BB-41 adsorption onto zeolite ZSM-5 at different initial concentrations.

C_0 mg.L^{-1}	Equations Y= A + B × X		R^2	K_p (mg.g^{-1}. min$^{-0.5}$)	$D_i/10^{-12}$ cm^2 s^{-1}
	A	B			
50	-1.58	0.78	0.739	0.78	1.206
100	-16.10	4.74	0.833	4.74	1.937
200	-23.40	8.27	0.915	8.27	2.109
300	-53.25	15.51	0.968	15.51	2.120

The values of the effective diffusion coefficient, were estimated to be of the order of 10^{-12} cm^2/s, indicating an adsorption process consisting of surface adsorption and pore diffusion. The regeneration tests indicated that the zeolite ZSM-5 had a stable reuse for three runs. Our findings provides a new insight into the designing an effective foam-shaped zeolite ZSM-5 for improving the adsorption capacity of basic blue. As a promising adsorbent for cationic dyes, the foam-shaped zeolite ZSM-5 may be a promising candidate to remove cationic pollutants from aqueous solutions in environmental pollution management.

REFERENCE

[1] Agnieszka, F.G., "Hierarchical zeolites: synthesis and catalytic properties." Micropor Mesopor Mater., 2018, 259, 33–45.

[2] Davis, R.J., "New perspectives on basic zeolites as catalysts and catalyst supports." Journal of Catalysis., 2003, 216,396– 405.

[3] Čejka, J, Centi G., Perez-Pariente, J. and Roth, W., "Zeolite-based materials for novel catalytic applications: Opportunities, perspectives and open problems." J. Catal. Today., 2012, 79, 2–15.

[4] Barthomeuf, D., "Basic zeolites: Characterization and uses in adsorption and catalysis". Catalysis Reviews. Science and Engineeringthis., 1996, 38,521– 612.

[5] Yun, J.L., Jin, S.L., Yong, S.P. and Kyung, B.Y., "Synthesis of large monolithic zeolite foams with variable macropore architectures." Adv. Mater., 2001, 13, 1259–1263.

[6] Vipin, K.S. and Joao, P., "Synthesis of foam-shaped nanoporous zeolite material: a simple template-based method." J.Chem. Educ., 2012, 89, 276–279.

[7] Xue, Z, Ma. J., Zhang, T., Miao, H. and Li, R., "Synthesis of nanosized ZSM-5 zeolite with intracrystalline mesopores." Mater. Lett., 2012, 68,1–3.

[8] Sarker, A.I., Aroonwilas, A. and Veawab, A., "Equilibrium and kinetic behaviour of CO_2 adsorption onto zeolites, carbon molecular sieve and activated carbons." Energy Procedia., 2017,114, 2450-2459.

[9] Elyssa, G.F., Darine, A.S., Severinne, S.R. and Daou, T.J., "Hierarchical zeolites as catalysts for biodiesel production from waste frying oils to overcome mass transfer limitaions." Molecules., 2021, 26, 4879.

[10] Ruh, U, Mohammed-Ali, H.S.S., Santiago, A. and Mert, A., "Adsorption equilibrium studies of CO_2, CH_4 and N_2 on various modified zeolites at high pressures up to 200 bar." Microporous Mesoporous Mater., 2018, 262, 49-58.

[11] Li, H.C., Ming-Hui, S., Zhao, W., Weimin, Y., Zaiku, X. and Bao-Lian, S., "Hierarchically structured zeolites: from design to application." Chemical Reviews., 2020, 120 (20), 11194-11294.

[12] Zhang, J, Wang, L., Ji, Y., Fang, C. and Feng-Shou, X., "Mesoporous zeolites for biofuel upgrading and glycerol conversion." Front. Chem. Sci. Eng., 2018, 12, 132–144.

[13] Tian-You, C, Rajendran, A., Hong-Xia, F., Feng, J. and Wen-Ying, L., "Review on hydro- desulfurization over zeolite-based catalysts." Industrial & Engineering Chemistry Research., 2021, 60(8), 3295-3323.

[14] Kabalan, I, Lebeau, B., Nouali, H., Toufaily, J., Hamieh, T., Koubaissy, B., Bellat J.P. and T. Daou J., "New generation of zeolite materials for environmental applications." J. Phys. Chem C., 2016, 120, 2688–2697.

[15] Laetitia, B, Maher, B.A., Simon-Masseron, A., Daou, T.J., Chaplais, G., Nouali, H., Schaf O., Zerega Y., Fiani E. and Patarin J., "Dioxin and 1, 2-dichlorobenzene adsorption in aluminosilicate zeolite Beta." Adsorption., 2017, 23, 101-112.

[16] Guillaume, R, Nouali, H., Daou, T.J., Faye, D. and Patarin, J., "Adsorption of volatile organic compounds in composite zeolites pellets for space decontamination." Adsorption, 2017, 23, 395-403.

[17] Xueping, S, Qin, Y., Mengyun, Y., Dan, T. and Limei, Z., "Highly efficient pollutant removal of graphitic carbon nitride by the synergistic effect of adsorption and photocatalytic degradation." RSC Advances., 2018, 8, 7260-7268.

[18] El-Hanache, L, Lebeau, B., Nouali, H., Toufaily, J., Hamieh, T. and Daou, T.J., "Performance of surfactant modified BEA-

type zeolite nanosponges for the removal of nitrate in contaminated water: Effect of the external surface." Journal of Hazardous Materials., 2019, 364,206-217.

[19] Xueshuai, C, Rongli, J., Yu, G., Zihan, Z. and Xingwen, W., "Synthesis of nano-ZSM-5 zeolite via a dry gel conversion crystallization process and its application in MTO reaction." Cryst. Eng. Comm., 2021, 23, 2793-2800.

[20] Ho, Y.S., Ng, J.C.Y. and McKay, G., "Kinetics of pollutant sorption by biosorbents. Review." Separation & Purification Reviews., 2000, 29, 189-232.

[21] Hermosin, M.C., Pavlovic, I., Ulibarri, M.A. and Cornejo, J., "Hydrotalcite as sorbent for trinitrophenol: Sorption capacity and mechanism." War. Res., 1996, 30,171-177.

[22] McCusker, L.B., "Zeolitecry stallography. Structure determination in the absence of conventional single-crystal data." Acta Cryst.A., 1991, 47, 297-313.

[23] Feng, R, Chen, K., Yan, X., Hu, X., Zhang, Y. and Wu, J., "Synthesis of ZSM-5 zeolite using coal fly ash as an additive for the methanol to propylene (MTP) reaction." Catalysts., 2019, 9, 788.

[24] Walton, K.S. and Snurr, R.Q., "Applicability of the BET method for determining surface areas of microporous metal-organic frameworks." J. Am. Chem. Soc., 2007, 129, 8552–8556.

[25] Pan, F, Lu, X., Wang, Y., Chen, S., Wang, T. and Yan, Y., "Organic template-free synthesis of ZSM-5 zeolite from coal-series kaolinite." Mater. Lett., 2014, 115, 5–8.

[26] Dmour, H.A., Kooli, F., Mohmoud, A., Liu, Y. and Popoola S.A., "Al and Zr Porous clay hetero structures as removal agents of basic blue-41 dye from an artificially polluted solution: regeneration properties and batch desig." Materials., 2021, 14, 2528.

[27] Kooli, F, Liu, Y., Abboudi, M., Oudghiri, H.H., Rakass, S., Sheikh, M.I. and Al-Wadaani, F., "Waste bricks applied as removal agent of basic blue 41 from aqueous solutions: base treatment and their regeneration efficiency." Appl. Sci., 2019, 9, 1237.

[28] Regti, A, Laamari, M.R., Stiriba, S. and El-Haddad, M. "Removal of basic blue 41 dyes using Persea americana-activated carbon prepared by phosphoric acid action." Int. J. Ind. Chem., 2017, 8, 187–195.

[29] Abul Hossain, M. and Mohibullah, M., "Kinetics and thermodynamics of adsoprtion of basic blue 41 on used black tea leaves." Int. J. Sci. Res., 2017, 8, 995–1002.

[30] Braja, N.P. and Deola, M., "Removal of anionic dyes from water by potash alum doped polyaniline: Investigation of kinetics and thermodynamic parameters of adsorption." J. Phys. Chem.B., 2015, 119, 8154–8164.

[31] Weihua, Z, Ke, L., Hongjuan, B., Xiaolan, S. and Runping, H., "Enhanced cationic dyes removal from aqueous solution by oxalic acid modified rice husk." J. Chem. Eng. Data., 2011, 56, 1882–1891.